Supplementary Information for

Differential Charging in Photoemission from Mercurated DNA Monolayers on Ferromagnetic Films

Dominik M. Stemer,[1,2] John M. Abendroth,[1,3,†] Kevin M. Cheung,[1,3] Matthew Ye,[1,3] Mohammed S. El Hadri,[4] Eric E. Fullerton,[4] and Paul S. Weiss[1,2,3,5*]

[1]California NanoSystems Institute, University of California, Los Angeles, Los Angeles, California 90095, United States

[2]Department of Materials Science & Engineering, University of California, Los Angeles, Los Angeles, California 90095, United States

[3]Department of Chemistry & Biochemistry, University of California, Los Angeles, Los Angeles, California 90095, United States

[4]Center for Memory and Recording Research, University of California, San Diego, La Jolla, California 92093, United States

[5]Department of Bioengineering, University of California, Los Angeles, Los Angeles, California 90095, United States

*Corresponding author: psw@cnsi.ucla.edu (PSW)

Supplemental Materials and Methods

Materials. Magnesium chloride, mercury (II) nitrate, absolute ethanol, and 6-mercapto-1-hexanoic acid (MHA) were purchased from Sigma-Aldrich (St. Louis, MO, USA). Phosphate-buffered saline (PBS, 0.01 M, [NaCl] = 138 mM, [KCl] = 2.7 mM, pH 7.4) was purchased from Thermo Fisher Scientific (Waltham, MA, USA). Deionized water (~18 MΩ) was obtained from a Millipore water purifier (Burlington, MA, USA).

All DNA sequences were purchased from Integrated DNA Technologies (IDT, HPLC-purified with a certificate of analysis *via* mass spectroscopy, Coralville, IA, USA). Sequences were modified with a propylthiol linker on the 3' terminus.

DNA sequences (5' → 3'):

0MM: TTT GTA AGA AGG CCC CCC TTC TTA CAA A

1MM: TTT GTT AGA AGG CCC CCC TTC TTA CAA A

2MM: TTT GTT TGA AGG CCC CCC TTC TTA CAA A

3MM: TTT GTT TGA AGG CCC CCC TTC TTT CAA A

7MM: TTT GTT TGT TGG CCC CCC TTC TTT CTT A

Fabrication, Characterization, and Surface Preparation of Ferromagnetic Multilayer Thin Films. The ferromagnetic multilayer (FM) thin films with perpendicular magnetization were grown on glass substrates by a DC magnetron sputtering system with a base pressure of $< 3\times10^{-8}$ Torr. These thin films are composed of glass substrate/Ta (3 nm)/Pt (2 nm)/[Co (0.6 nm)/Pt (0.3 nm)]$_{69}$/Co (0.6 nm)/Au (2 nm).[S1] The deposition was performed at room

temperature and in an Ar gas atmosphere. The Ar pressure during the sputter deposition was 10 mTorr for the Co and Pt layers and 2.7 mTorr for the Ta and Au layers.

The FM thin films were characterized using the vibrating sample magnetometer (VSM) option of a VersaLab system (Quantum Design, Inc., San Diego, CA, USA). Samples were mounted within translucent plastic straws. The applied magnetic field was perpendicular to the samples plane. Hysteresis loops were slope-corrected for diamagnetic responses from the substrates by subtracting the constant slope at high field from each dataset. The ferromagnetic films exhibit perpendicular magnetic anisotropy with large room-temperature coercive fields of 3350 Oe (Figure S1).

Prior to functionalization, FM substrates were magnetized within a SQUID magnetometer (Quantum Design, Inc.) by applying a magnetic field perpendicular to the plane of the surface. Samples were magnetized to saturation under an applied field of +12 kOe or -12 kOe for samples considered to be magnetized up or down, respectively. Immediately preceding functionalization, magnetized substrates were sonicated sequentially for 10 min in acetone and ethanol before being dried with N_2.

Ferromagnetic Multilayer Thin Film Surface Functionalization. Fresh 5 μM DNA solutions were prepared in degassed 1× PBS containing 100 mM $MgCl_2$ during each instance of sample fabrication. For mercurated sequences, aqueous $Hg(NO_3)_2$ was added to reach a final concentration of 5 μM (1MM) or 35 μM (7MM), depending on the DNA sequence. These solutions were allowed to stand for 30 min at room temperature to allow for mercury incorporation into the thymine-thymine mismatches within the hairpin sequences (Figure S2a,b).

Self-assembled monolayers (SAMs) of DNA were prepared by incubating clean FM substrates with DNA solutions for 48 h in a hydrated environment by pipetting solution onto individual FM substrates and sealing in petri dishes. Following monolayer formation, substrates were thoroughly rinsed with DI water before subsequent incubation in 1 mM ethanolic solutions of MHA for 20 min. Substrates were then rinsed with ethanol and DI water and blown dry with N_2.

Melting Curve Analysis. Solutions of 5 μM non-thiolated DNA were prepared in 1× PBS using the sequences listed above. For mercurated sequences, aqueous $Hg(NO_3)_2$ was added to reach a final concentration of 5 μM (0MM, 1MM), 10 μM (2MM), 15 μM (3MM), or 35 μM (7MM), depending on the sequence. Solutions were allowed to stand for 30 min at room temperature prior to measurement.

Measurements were taken with a JASCO J-815 circular dichroism spectrometer (Easton, MD, USA). For each condition, N = 3 samples were independently prepared and measured. The temperature increment was 2.0 °C and the delay time was 60 s. Absorbance values were collected at 260 nm for all solutions. Data presented in Figures 2g-i and S2e,f were normalized using the standard relation $[Abs_{260\,nm}(T) - Abs_{260\,nm}(25\,°C)] / [Abs_{260\,nm}(85\,°C) - Abs_{260\,nm}(25\,°C)]$. Shaded areas represent standard error of the mean.

Circular Dichroism Spectroscopy. Solutions of 5 μM non-thiolated DNA were prepared in 1× PBS using the sequences listed above. For mercurated sequences, aqueous $Hg(NO_3)_2$ was added to reach a final concentration of 5 μM (0MM, 1MM) 10 μM (2MM), 15 μM (3MM), or 35 μM (7MM), depending on the sequence. Solutions were allowed to stand for 30 min at room temperature prior to measurement.

Measurements were taken with a JASCO J-815 circular dichroism spectrometer (Easton, MD, USA) at 25 °C. For each condition, N = 3 samples were independently prepared and measured. The resolution was 0.5 nm, the bandwidth was 1.0 nm, the response time was 4 s, and the collection speed was 50 nm/min. Shaded areas represent standard errors of the mean. Characterization of DNA mismatches with intermediate numbers of T-T mismatches (2MM and 3MM) are shown in Figure S2.

Surface Characterization by X-Ray Photoelectron Spectroscopy. X-ray photoelectron spectroscopy of all samples was done using an AXIS Ultra DLD photoelectron spectrometer (Kratos Analytical Inc., Chestnut Ridge, NY, USA) and a monochromatic Al K_α X-ray source with a 200 μm circular spot size under ultrahigh vacuum (10^{-9} Torr). All samples were grounded by copper clips in contact with the top surfaces of each substrate, and tightly secured onto the sample holder with copper screws. The heights of all samples were optimized prior to spectral acquisition to maximize the signal to noise. High resolution Hg 4f spectra were acquired at a pass energy of 20 eV using a 300 ms dwell time (Figure S3). For all scans, 15 kV was applied with an emission of 15 mA. An average of 20 scans were collected for each high-resolution spectrum.

Surface Characterization by Ultraviolet Photoelectron Spectroscopy. An AXIS Ultra DLD photoelectron spectrometer (Kratos Analytical Inc., Chestnut Ridge, NY, USA) and a He I excitation source (21.22 eV) was utilized under a -9 V bias between the samples and detector during sample characterization. All samples were grounded by copper clips in contact with the top surfaces of each substrate and secured in place with copper screws. Spectra were acquired at a pass energy of 5 eV with a 100 ms dwell time and a slot aperture. Sample heights were optimized using the Au 4f signal in order to maximize signal to noise prior to measurement. For each sample, three spectra were collected, each at different locations. Measurements were collected alternatively from

samples magnetized up or down. The angle of incidence for UV irradiation was 35° relative to the plane of the surface. Photoelectrons were collected normal to the sample surface.

The energies of the binding edge maxima and minima were measured at the x-intercepts of the maximum slopes at the spectral fringes using linear fits to the data prepared with a custom Python script. For each sample, the ionization energy or work function values were extracted from each of three measurements taken at different locations and were averaged together into a single value (Figure 3e-g, S4). The average ionization energies or work functions for each sample were then averaged across the total number (N) of samples of the same type, and the mean and standard error recorded. Representative profile fits are shown in Figure S5.

Statistics. Data analyses were performed with GraphPad Prism (GraphPad Software Inc., San Diego, CA, USA). Probabilities $P < 0.05$ were considered statistically significant, and throughout the main text and Supplementary Information, data are reported as mean values ± standard errors of the mean. Two-tailed, unpaired *t*-tests were used to compare photoionization energies between magnetization up and down conditions 0MM and 7MM + Hg^{2+} samples. Two-way analysis of variance was used to identify differences in work function and ionization energy between 1MM samples prepared in the presence or absence of Hg^{2+}, under both up and down magnetization conditions. Two-way analysis of variance was followed by Bonferroni *post hoc* tests (Tables S1, S2).

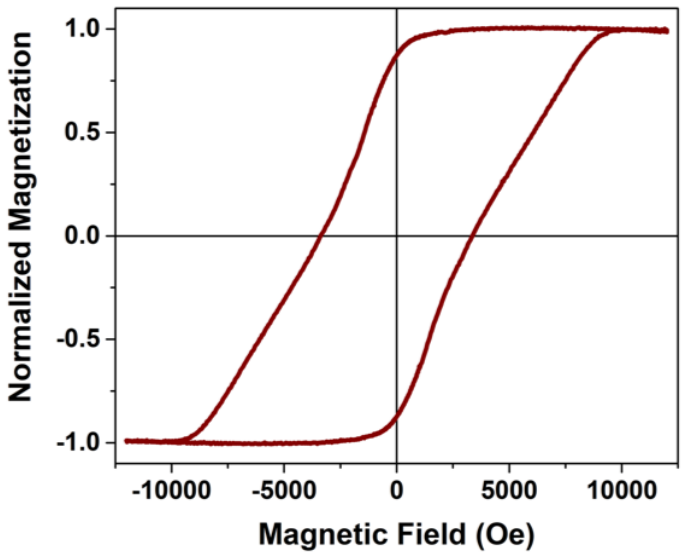

Figure S1: Room temperature SQUID magnetic hysteresis loop of the ferromagnetic substrates used in these studies. The applied magnetic field is perpendicular to the film plane. This hysteresis loop represents a ferromagnetic film with robust perpendicular magnetic anisotropy. The high (~3 kOe) coercivities were necessary to maintain substrate magnetization fidelity within the magnetic focusing lens of the photoelectron spectrometer.

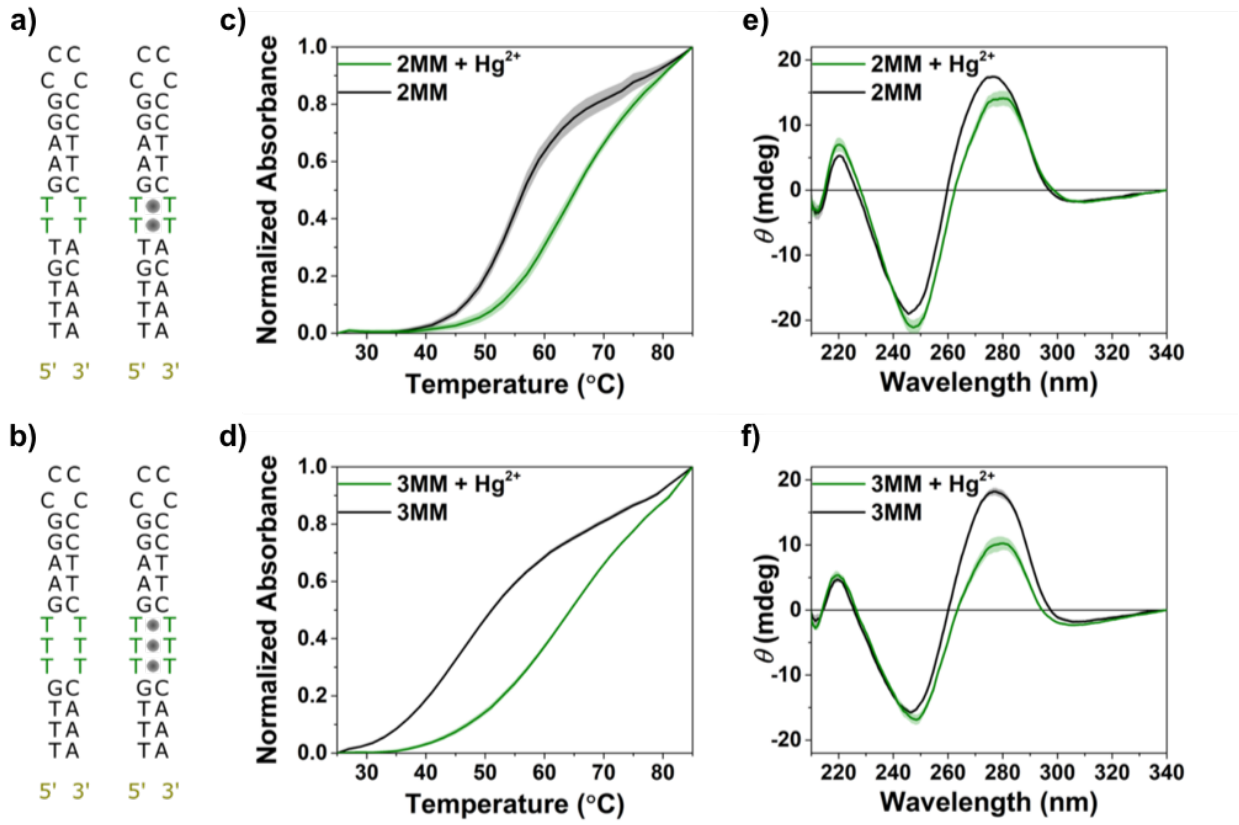

Figure S2: Characterization of DNA sequences with intermediate numbers of thymine-thymine mismatches (MM). **a,b)** Schematics of 2MM and 3MM DNA, respectively, illustrating number of thymine-thymine mismatches (left), and of the same sequences in the presence of Hg^{2+} ions (right). **c,d)** Melting curves for 2MM and 3MM DNA. Peak absorbance at 260 nm is normalized to the maximum value for each curve. **e,f)** Circular dichroism spectra for 2MM and 3MM. Melting curves and circular dichroism were collected for each sequence in the presence (green) or absence (black) of stochiometric Hg^{2+}. The concentration of all DNA solutions was 5 μM.

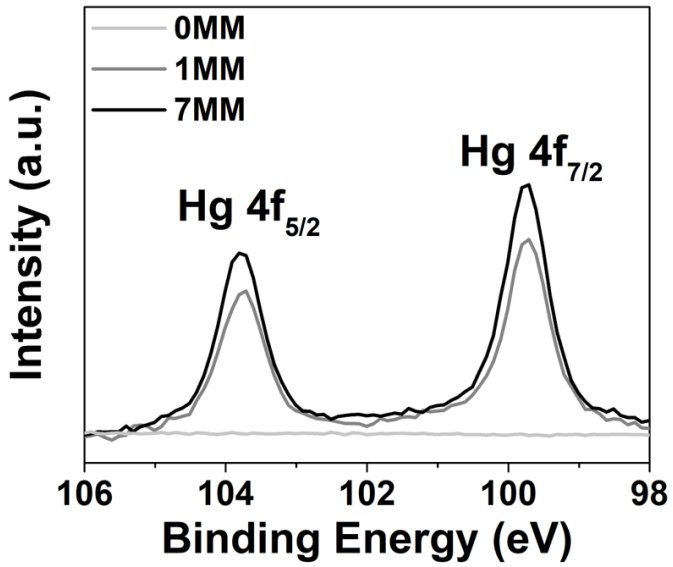

Figure S3: X-ray photoelectron spectroscopy of self-assembled monolayers of DNA with no thymine-thymine mismatches (0MM, light gray), 1MM (dark gray), and 7MM (black) on ferromagnetic substrates prepared in the presence of stochiometric concentrations of Hg^{2+} ions. Two-tailed, unpaired *t*-tests indicate that the atomic percentage of Hg in samples of 7MM is significantly greater than that found in 1MM ($P < 0.01$, $N = 2$).

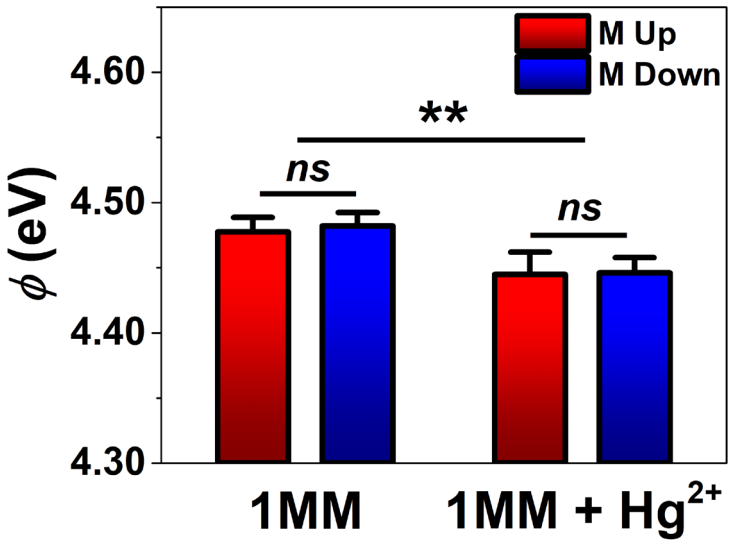

Figure S4. Work function values collected under up (red) and down (blue) substrate saturation magnetization conditions for self-assembled monolayers of DNA with one thymine-thymine mismatch with (left) and without (right) one equivalent of Hg^{2+}. Error bars represent standard error of the mean. Number of samples (N) = 20 [1MM Up], 20 [1MM Down], 20 [1MM + Hg^{2+} Up], 20 [1MM + Hg^{2+} Down]. $^{**}P < 0.01$ vs Hg^{2+}; *ns* = not significant.

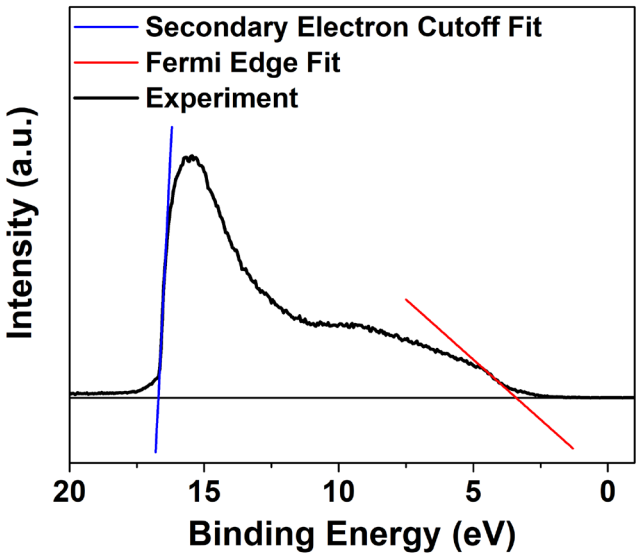

Figure S5: Representative linear fit to the absolute maximum slope used for determination of binding edge maxima (blue) and minima (red).

Table S1: Two-way analysis of variance (ANOVA) results for ionization energy in DNA with 1 thymine-thymine mismatch (1MM) with main effects of mercury incorporation and magnetization orientation. Bonferroni post-hoc tests analyzing the role of mercury incorporation in the manifestation of magnetization-dependent ionization energy.

Ionization Energy (1MM)

	Interaction	**Mercuration**	**Magnetization**
	F (1, 76) = 4.597	F (1, 76) = 156.1	F (1, 76) = 4.958
	$P = 0.0352$	$P < 0.0001$	$P = 0.0289$
	No Hg	**Hg**	
Bonferroni (Up-Down)	$P > 0.9999$	$P = 0.0056$	

Table S2: Two-way analysis of variance (ANOVA) results for work function in DNA with 1 thymine-thymine mismatch (1MM) with main effects of mercury incorporation and magnetization orientation. Bonferroni post-hoc tests analyzing the role of mercury incorporation in the manifestation of magnetization dependent work function.

Work Function (1MM)

	Interaction	**Mercuration**	**Magnetization**
	F (1, 76) = 0.01726	F (1, 76) = 7.055	F (1, 76) = 0.04839
	$P = 0.8958$	$P = 0.0096$	$P = 0.8265$
	No Hg	**Hg**	
Bonferroni (Up-Down)	$P > 0.9999$	$P > 0.9999$	

Table S3: Summary of sample number (*N*), and ionization energy, work function, and photoelectron spectra integrated area and peak intensity for all samples studied. Uncertainty is represented as standard error of the mean (SEM).

	0MM Up	**0MM Down**	**1MM Up**	**1MM Down**	**1MM + Hg Up**	**1MM + Hg Down**	**7MM + Hg Up**	**7MM + Hg Down**
N	19	19	20	20	20	20	19	20
Ionization Energy (eV)								
mean	7.70	7.70	7.84	7.83	7.72	7.67	7.87	7.91
SEM	1×10^{-2}	1×10^{-2}	1×10^{-2}	1×10^{-2}	1×10^{-2}	1×10^{-2}	1×10^{-2}	1×10^{-2}
Work Function (eV)								
mean	4.51	4.53	4.48	4.48	4.44	4.45	4.47	4.49
SEM	1×10^{-2}	1×10^{-2}	1×10^{-2}	1×10^{-2}	2×10^{-2}	1×10^{-2}	1×10^{-2}	1×10^{-2}
Integrated Area								
mean	9.11×10^{6}	7.99×10^{6}	7.72×10^{6}	$8.36\text{E}\times10^{6}$	7.94×10^{6}	6.60×10^{6}	7.50×10^{6}	8.01×10^{6}
SEM	8.1×10^{5}	2.46×10^{6}	1.36×10^{6}	1.88×10^{6}	9.3×10^{5}	2.19×10^{6}	8.5×10^{5}	1.24×10^{6}
Peak Intensity								
mean	8.12×10^{4}	7.19×10^{4}	7.11×10^{4}	7.62×10^{4}	7.03×10^{4}	5.91×10^{4}	7.35×10^{4}	7.69×10^{4}
SEM	8.2×10^{3}	2.22×10^{4}	9.8×10^{3}	1.35×10^{4}	7.8×10^{3}	2.01×10^{4}	7.8×10^{3}	1.16×10^{4}

Reference

(S1) Honda, S.; Tanimoto, H.; Kusuda, T. Magnetization Process and Coercivity of Sputtered Co/Pt Multilayered Films. *IEEE Trans. Magn*. **1990**, *26*, 2730–2732.